Physical Modelling in Geotechnics

Assessment of boundary effects of the Equivalent Shear Beam container for dynamic centrifuge testing of liquefiable soils

D. Gaudio
Dipartimento di Ingegneria Strutturale e Geotecnica, Sapienza Università di Roma, Rome, Italy

J. Seong, S.K. Haigh, G. Viggiani & G.S.P. Madabhushi
Department of Engineering, University of Cambridge, Cambridge, UK

ABSTRACT: Centrifuge modelling is a widely-used tool to assess the response of reduced-scale structures subjected to earthquakes under an increased gravity environment. Indeed, this experimental technique allows the user to obtain experimental results under repeatable and controlled conditions. However, space limitations force the model to be constrained into relatively small containers, such as the laminar and Equivalent Shear Beam (ESB) containers. In this paper, the influence of the proximity of the ESB box boundaries adopted for dynamic centrifuge tests at Schofield Centre, University of Cambridge, is evaluated: the example case of an Onshore Wind Turbine resting on saturated sandy soils, for which liquefaction was triggered during seismic events, is considered. Numerical modelling of the ESB box was implemented in the Finite Element framework OpenSees, to capture the experimental results: hydro-mechanical soil parameters were first calibrated against far-field centrifuge results only. From this calibration, the seismic performance of the raft foundation turned out to be in a good agreement with the experimental results, for a moderate-intensity sinusoidal input representing ground motions capable of triggering liquefaction. Then, a larger numerical model was built, where boundaries do not play significant role. This allowed outcomes to be compared with those resulting from the smaller model. This way, the effect of ESB boundaries was assessed by comparing both the far-field soil and the structure response induced by two sine waves with different intensities, both triggering liquefaction.

Keywords: Wind Turbine, Liquefaction, Dynamic centrifuge testing, 3D Finite Element Analyses, OpenSees.

1 INTRODUCTION

Centrifuge modelling is a well-known and powerful technique which can be profitably adopted when dealing with Dynamic Soil-Structure Interaction (DSSI) problems, especially when evaluating the performance of a structure subjected to strong seismic events. The widespread use of centrifuge testing can be mainly ascribed to some advantageous features characterising this tool, such as the possibility to study the dynamic response of reduced-scale models without needing any assumption on soil behaviour, and to make the soil sample under repeatable and controlled conditions (*e.g.*, 1D consolidation of clay samples, Gaudio *et al.* (2022a)).

The above-mentioned advantages are particularly effective when assessing the liquefaction hazard to structures on loose, superficial sandy soils. These benefits make dynamic centrifuge tests also attractive when calibrating complex numerical Finite Element (FE) 3D models, which can then be used to perform extensive parametric studies (Chen *et al*., 2021).

Dynamic centrifuge tests may be adversely affected by the presence of the boundaries of the container where the reduced-scale model is placed into, such as the Laminar or Equivalent Shear Beam (ESB) boxes, which are characterised by constrained dimensions. Although these model containers are designed to minimise the boundary effects in dynamic centrifuge tests, the close boundaries can generate some P-waves that remain trapped in the container, which may reduce the geometric (radiation) damping that actually plays a fundamental role in the seismic performance in the field. With particular reference to an older version of the ESB container, Teymur and Madabhushi (2003) showed that this unfavourable phenomenon is maximised when the stiffness contrast between the soil sample and the end walls is high, which is definitely the case for sandy soils where liquefaction is triggered due to strong earthquakes.

Recently, Gaudio *et al*. (2022b) assessed the boundary effects of the most recent ESB box (Brennan and Madabhushi, 2002) available at the Schofield Centre, University of Cambridge, referring to the seismic performance of an Onshore Wind Turbine (OWT) resting on a liquefiable soil deposit. A centrifuge test was first performed, where the reduced-scale model was subjected to a series of base excitations, both theoretical (*e.g.* sine waves) and real ground motions. Then,

advanced 3D numerical simulations were performed in the OpenSees FE framework v. 3.3.0 (McKenna *et al*., 2000; Tarque Ruiz, 2020) through a *small* model, characterised by the same dimensions (at prototype scale) as those of the ESB box, to accurately replicate the results obtained in the centrifuge. In the FE analyses, mechanical soil behaviour under cyclic loading was described via the SANISAND04 model (Dafalias and Manzari, 2004), and the two-phase nature of soils was explicitly considered through the *u-p* formulation (Zienkiewicz *et al*., 1980). Calibration of hydro-mechanical soil parameters against the far-field soil response was needed at this stage. Then, a *large* numerical model, where the structure was not affected by the presence of lateral boundaries, was implemented: the outcomes obtained with the latter FE model were compared with those coming from the *small* one, so as to assess the influence of boundaries.

In this paper, some new results obtained with two sine waves characterised by a different intensity are presented and discussed, stressing that boundary effects are less dependent on the seismic amplitude, provided that liquefaction is triggered. The schematic layout considered in the study is depicted in Fig. 1, where an OWT of height h_s = 48 m rests on a circular raft foundation with diameter D = 15.4 m and thickness s = 1.6 m. The tower is characterised by a total mass m_{tot} = 435.8 Mg and a fixed-base natural frequency $f_s \approx 0.3$ Hz, while the raft foundation rests on a fully-saturated loose sand layer (relative density D_R = 43 %) of thickness 15 m, underlain by a dense sand layer (D_R = 90 %) of thickness 12 m. The average contact pressure exerted by the structure is q = 58.8 kPa.

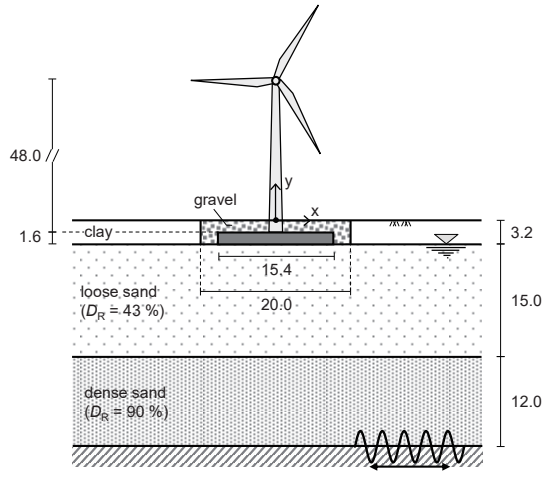

Fig. 1. Schematic layout of the problem (dimensions in meters).

The surface layer consists of a 3.2 m-thick partially-excavated clay, replaced with gravel close to the foundation. The water table is located at the gravel/clay-loose sand contact, with a hydrostatic initial pore water pressure regime. The system is subjected at the base, in the horizontal x-direction, to seismic motions intense enough to trigger liquefaction.

2 DYNAMIC CENTRIFUGE TEST

The scaled model of the OWT was made to reproduce the layout depicted in Fig. 1 and test it with the 10-m-diameter Turner beam centrifuge at University of Cambridge, UK. The model was spun at a nominal centrifugal acceleration of 80*g*. In the model, the OWT is represented through a steel hollow tube with a brass mass, the latter simulating the weight of the rotor, blades, generator and all pieces of equipment at the tip, while the raft foundation is reproduced by a circular aluminium plate. At model scale, the steel hollow tube has an outer diameter of 17.5 mm (1.4 m at prototype scale) and a wall thickness equal to 2.5 mm (0.2 m), and the foundation has a diameter of 192 mm and a thickness of 20 mm, following the scaling laws of centrifuge testing. The lumped brass mass is m_{lump} = 300 g (153.6 Mg).

The layers of sand, clay and gravel were created in three steps. First, the sand layers were put in the model container through the automatic sand pourer available at the Schofield Centre. Then, the clay layer was made using pre-cut clay blocks. Finally, the gravel was placed in the gap where the raft foundation was located. As for the sand layers, Hostun HN31 sand was adopted, whose physical properties are listed in Table. 1, where G_s is the specific gravity, e_{max} and e_{min} are the maximum and minimum void ratio, respectively, and φ'_{cv} is the constant-volume friction angle. The target relative densities were first achieved by air pluviation; then, the sand layers were fully-saturated through the aqueous solution of hydroxypropyl methylocellulose with a viscosity of 80 MPa·s.

A picture of the model is given in Fig. 2. The model was equipped with miniaturised instrumentation, including piezo-electric accelerometers (piezos) and Micro-Electrical-Mechanical-Systems (MEMS) to record the acceleration time histories, Pore Pressure Transducers (PPTs) for the pore water pressures and Linear Variable Differential Transformers (LVDTs), the latter to measure vertical displacements of the raft foundation and therefore its rigid rotation. The model was also equipped with an Air Hammer Device to provide the profiles of the soil shear wave velocity. A more detailed presentation of the adopted instrumentation is given in Gaudio *et al*. (2022b).

Table 1. Physical properties of Hostun sand HN31

G_s (-)	e_{max} (-)	e_{min} (-)	φ'_{cv} (°)
2.65	1.011	0.555	33

Fig. 2. Reduced-scale model loaded on the centrifuge.

3 3D FINITE ELEMENT ANALYSES

After performing the centrifuge test, an extensive numerical parametric study was carried out to assess the boundary effects of the ESB container. To this end, 3D nonlinear dynamic FE analyses were performed in the time domain, implementing 3D models in the OpenSees framework. Unless otherwise stated, all dimensions in the following are given at prototype scale.

First, a *small* model was developed, aimed at representing the reduced-scale model tested in the centrifuge but at prototype scale. Specifically, the dimensions of the *small* numerical model are exactly those characterising the ESB container, namely $X = 51.6$ m ($\approx 3.4 \times D$), $Z = 9.12$ m ($\approx 1.2 \times D/2$) and $Y = 30.2$ m ($\approx 2 \times D$), taking advantage of symmetry of the problem. The FE mesh of the *small* model is composed of 2401 elements and 3121 nodes, with a progressively finer mesh approaching the raft foundation (shaded volume in Fig. 3). *BrickUP* elements were assigned to the whole domain, which are hexahedral linear isoparametric FEs characterised by 8 nodes with 4 degrees of freedom each, three for solid displacements and one for fluid pressure, and by 8 stress points. The tower was modelled through Timoshenko *beam* elements to consider the shear deformability of the tower, with a tip lumped mass.

In the initial static (gravity) calculation phase, standard boundary conditions were applied to the model, *i.e.*, $u_x = 0$ along the lateral y-z boundaries, $u_z = 0$ along the x-y boundaries and fixed nodes at the base of the mesh ($u_x = u_y = u_z = 0$). When switching to the dynamic calculation phase, the restraints on the horizontal displacements at the base of the mesh were removed and periodic constraints were applied to the nodes along the vertical x-z boundaries ($\Delta u_x = 0$). The latter is equivalent to the free-field pure-shear conditions applied by the end walls of the ESB container. Hydraulic boundary conditions were set up with the water table located at the top of the loose sand: pore water pressures were allowed to fluctuate freely for all nodes within the sand layers ($y \leq$ -3.2 m), while both steady and excess pore water pressures were inhibited in the clay and gravel layers ($p = \Delta p = 0$). Several base excitations, identical to those applied in the centrifuge, were imposed at the base of the system: however, in this paper the results coming from two of them only are discussed. These are a moderate and high-intensity sinusoidal acceleration time history, characterised by the same frequency, $f = 1$ Hz, and total duration, $T_f = 10$ s, but different peak acceleration during its stationary part, $a_g = 0.20$ and 0.25 g.

Mechanical behaviour of soils was simulated through the Pressure Independent Multi-Yield (PIMY) model for the clay, the Pressure Dependent Multi-Yield (PDMY) for the gravel and SANISAND04 for the sand layers. As for the clay and gravel layer, typical values provided by Yang *et al*. (2008) for a soft clay and medium dense sand were adopted, while the hydro-mechanical sand parameters were calibrated against the acceleration and pore water pressure build-up recorded along the far-field alignment (Fig. 4), as discussed in Gaudio *et al*. (2022b).

The same analyses were performed with the *large* model (Fig. 3), whose results are clearly not affected by the presence of vertical boundaries. The FE model is now made of 12013 elements and 13780 nodes.

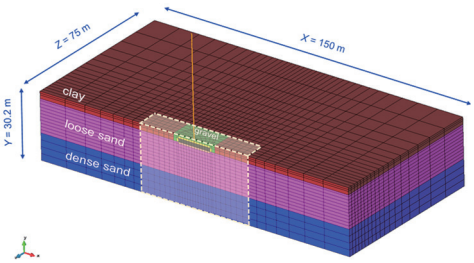

Fig. 3. *Large* and *small* (shaded volume) 3D FE models.

The seismic performance of the raft foundation is given in Fig. 4 for the moderate intensity sine wave ($a_g = 0.20$ g), where the time histories of the average raft settlement w, relative to the far-field w_{ff}, is plotted (Fig. 4d), together with the raft rigid rotation θ (e). In the same Figure, the absolute settlements at the far-field w_{ff} (a) and at both foundation sides (b-c) are plotted. From the comparison of the experimental results (blue lines) with the ones obtained with the *small* FE model (red lines), it turns out that the calibration of hydro-mechanical sand parameters provided quite a satisfactory estimation of the both the far-field and raft response. Conversely, the comparison with the results coming from the *large* model shows that both the peak relative settlement and rotation of the raft decrease, going from 0.42 to 0.31 m and from about 0.20° to 0.12°, respectively (Table. 2).

From a rigorous point of view, these differences are not negligible, which demonstrate that the ESB boundaries do affect the seismic performance of the raft (and therefore, of the OWT). However, the observed difference in the raft rotation is less than 0.1°, which is modest if compared with the threshold rotations of about 0.50 - 0.75°, typically allowed for wind turbines. Moreover, the estimation provided by the *small* FE model (and therefore, by the centrifuge test) turned out

to be on a safer side, providing higher values of the raft settlement relative to the far-field. It is worth mentioning that the observed difference in terms of settlement is to be attributed to the absolute far-field settlement w_{ff} (Fig. 4a) rather than to the absolute settlements of both sides of the raft (Fig. 4b-c), whose numerical prediction is not affected by the presence of the boundaries. In fact, the far-field settlement w_{ff} is almost null when the boundaries are far away (i.e., *large* FE model), whereas is negative (heave) in the close presence of the boundaries (i.e., *small* FE model). For the sake of brevity, the time histories obtained for the high-intensity sine wave (a_g = 0.25 g) are not shown here. However, the resulting peak values are provided in the next section.

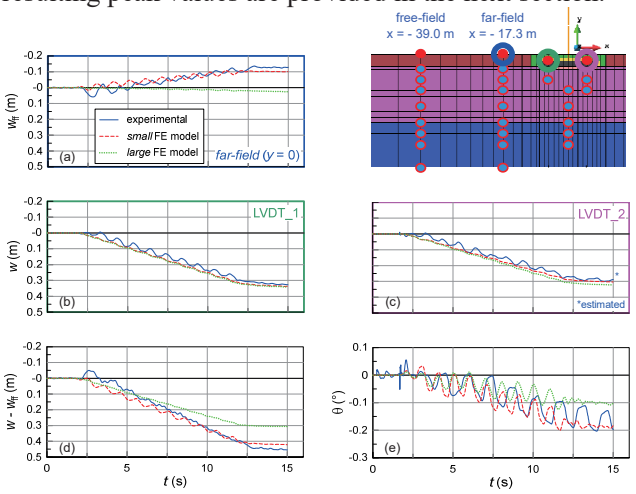

Fig. 4. Settlement time histories of (a) far-field and (b-c) foundation sides, together with the (d) average relative settlement and (e) rotation of the raft foundation (a_g = 0.20g).

4 ASSESSMENT OF BOUNDARY EFFECTS

The ESB boundary effects are quantified through some seismic performance indexes, such as the peak values of the relative settlement, $(w - w_{ff})_{max}$, and of the rigid rotation of the raft, θ_{max}, obtained with the *small* and *large* FE model when applying the two sine waves. These peak values are plotted in Fig. 5 and listed in Table.2. It can be readily recognised that about the same differences already discussed for the moderate-intensity sine wave are obtained for the high-intensity input, when switching from the *small* to the *large* 3D FE model, both for the relative settlement and rotation of the raft. This suggests that the ESB boundary effects do not depend on the seismic input amplitude, provided that the base excitation is intense enough to trigger liquefaction in the liquefiable sand deposit.

5 CONCLUSIONS

In this paper, the boundary effects induced by end walls of the ESB container adopted at University of Cambridge have been assessed, referring to the case of an OWT resting on a soil deposit for which liquefaction is triggered, due to both a moderate and high-intensity sine waves. The results discussed show that the boundaries only slightly affect the seismic performance of the raft, here expressed in terms of permanent settlement and rotation, providing a safe estimation of these performance indexes. The discussion of results shed some light on the role of the ESB flexible boundaries in the presence of a high stiffness contrast between the soil sample and the wall ends, thus permitting to gain more awareness of results coming from centrifuge tests.

Table 2. Seismic performance indexes obtained in the FE analyses

a_g (g)	$(w\text{-}w_{ff})_{max}$ (m)		θ_{max} (°)	
	small	*large*	*small*	*large*
0.20	0.42	0.31	0.20	0.12
0.25	0.53	0.43	0.14	0.07

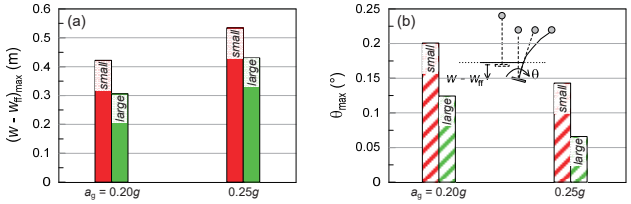

Fig. 5. Seismic performance indexes obtained with the *small* and *large* FE models for different seismic intensities.

REFERENCES

Brennan A.J. and Madabhushi S.P.G. 2002. Design and performance of a new deep model container for dynamic centrifuge testing. *Proc. Int. Conf. Phys. Mod. Geotech.*, Balkema, Rotterdam, 183-188.

Chen L., Ghofrani A. and Arduino P. 2021. Remarks on numerical simulation of the LEAP-Asia-2019 centrifuge tests. *Soil Dyn. Earthq. Eng.* 142, 106541.

Dafalias Y.F. and Manzari M.T. 2004. Simple plasticity sand model accounting for fabric change effects. *J. Eng. Mech. ASCE* 130 (6), 622-634.

Gaudio D., Madabhushi S.P.G., Rampello S., Viggiani G.M.B. 2022a. Experimental Investigation of the seismic performance of caisson foundations supporting bridge piers. *Géotechnique*.

Gaudio D., Seong J., Haigh S.K., Viggiani G.M.B., Madabhushi S.P.G., Shrivatsava R., Veluvolu R. and Padhy P. 2022b. Boundary effects on dynamic centrifuge modelling of onshore wind turbines on liquefiable soils, *Int. J. Phys. Mod. Geotech* (*in press*), https://doi.org/10.1680/jphmg.21.00085 .

McKenna F., Fenves G.L., Scott M.H. and Jeremić B. 2000. *Open system for earthquake engineering simulation*. http:// opensees.berkeley.edu

Tarque Ruiz S.N. 2020. Programa compilado OpenSees, mayo 2020. PERU.

Teymur B. and Madabhushi S. P. G. 2003. Experimental study of boundary effects in dynamic centrifuge modelling. *Géotechnique* 53 (7), 655-663.

Yang Z., Lu J. and Elgamal A. 2008. *OpenSees soil models and solid-fluid fully coupled elements: User's manual*. San Diego: Dept. of Structural Engineering, Univ. of California.

Zienkiewicz O.C., Chang C.T. and Bettes P. 1980. Drained, undrained, consolidating and dynamic behaviour assumptions in soils. *Géotechnique* 30 (4), 385-395.